applied sciences

MDPI

Article

Experimental Investigation of the Cooling Effect Generated by a Heat Sink Integrated Thermoelectric-Based U-Shaped Air-Conditioning System

Yesha Patel, Abu Raihan Mohammad Siddique, Mohammad Reza Mohaghegh *, Syeda Humaira Tasnim and Shohel Mahmud

School of Engineering, University of Guelph, Guelph, ON N1G 2W1, Canada; yeshapatel95@gmail.com (Y.P.); asiddi04@uoguelph.ca (A.R.M.S.); stasnim@uoguelph.ca (S.H.T.); smahmud@uoguelph.ca (S.M.)
* Correspondence: mohaghem@uoguelph.ca

Abstract: Over the past years, thermoelectric refrigeration has attracted considerable attention due to its compact size, reliability, and environmental friendliness. Traditional refrigeration systems use greenhouse gases, which significantly impacts our environment. Therefore, in this work, a thermoelectric cooler prototype refrigeration system, a solid-state device causing no harm to the environment, was constructed and tested experimentally. A heat sink was attached to the cold side of the thermoelectric cooler (TEC) to cool the air passing through the heat sink. In contrast, a cold plate was attached to the hot side of TEC to remove the generated heat with the help of the liquid circulating in the aluminium cold plate. Experiments were carried out by varying parameters such as input current to the TEC module, inlet air flow rate, water flow rate through the cold plate, etc. The experimental results indicate that the cooling effect is increased by approximately 40%, increasing current from 2A to 8A. However, the cooling effect was decreased with increasing inlet airflow rate by 58% when airflow rate increased from 2.25 m/s to 3.55 m/s. However, the system performance shows approximately 35% increment with an increase in fan speed. Furthermore, a decrease in the water flow rate from 3.04 L/m to 1.80 L/m showed a slight increment in the cooling by 15%.

Keywords: air-conditioning; bulk mean temperature; coefficient of performance (COP); heat removal rate; thermoelectric cooler

check for updates

Citation: Patel, Y.; Siddique, A.R.M.; Mohaghegh, M.R.; Tasnim, S.H.; Mahmud, S. Experimental Investigation of the Cooling Effect Generated by a Heat Sink Integrated Thermoelectric-Based U-Shaped Air-Conditioning System. *Appl. Sci.* **2021**, *11*, 10288. https://doi.org/10.3390/app112110288

Academic Editors: Mingke Hu and Qiliang Wang

Received: 21 September 2021
Accepted: 31 October 2021
Published: 2 November 2021

Publisher's Note: MDPI stays neutral with regard to jurisdictional claims in published maps and institutional affiliations.

Copyright: © 2021 by the authors. Licensee MDPI, Basel, Switzerland. This article is an open access article distributed under the terms and conditions of the Creative Commons Attribution (CC BY) license (https://creativecommons.org/licenses/by/4.0/).

1. Introduction

Refrigeration has a wide range of engineering applications such as air-conditioning, perishable food refrigeration, electronic cooling, chemical and process engineering and medical science [1]. The required chilled liquid divides the refrigeration process into three categories: (i) absorption refrigerator systems, (ii) vapor compression refrigerator systems, and (iii) special refrigerator systems using the thermoelectric effect. Conventional refrigeration systems use a vapor compression system having a high coefficient of performance (COP), however, they uses toxic chemicals such as chlorofluorocarbons (CFCs), which significantly affect global warming. Therefore, researchers are focusing on developing new, environmentally friendly techniques for refrigeration and cooling air [2].

Thermoelectric refrigeration, also known as a thermoelectric cooler (TEC), is an environmentally friendly technique that uses thermoelectric modules, solid-state heat pumps that work on the Peltier effect. The devices generate a cooling effect when a certain voltage is applied to the appropriate direction across the junctions. TEC has several advantages such as no mechanical moving parts, light in weight, compact in size, lower noise and vibration, good temperature control, and no fluid involvement [3,4]. Furthermore, they be powered by a direct current (DC) power supply such as photovoltaic (solar energy) and fuel cells [1]. Recently, researchers have been investigating the performance of TE system using solar cells to minimize the load on the regular power supply and save energy [1].

Generally, two sinks are attached to the hot and cold side of the module to improve the system performance and heat transfer rate of TEC [2]. Thermoelectric cooling technology covers a wide range of application areas, including refrigeration, electronic and automobile cooling, thermoelectric air-conditioning, freshwater production, etc. For thermoelectric cooling system design, there are two important parameters: the cooling power and the coefficient of performance (COP). The COP of the thermoelectric module significantly affects the COP of the overall system. There are several techniques to enhance the performance of the thermoelectric cooling system which can be categorized as thermal design, thermoelectric module design, and operating design of the thermoelectric cooling system. Vapor compression systems, however, have better COP and are more reliable, even though they have moving parts (but require very little maintenance) [5]. Furthermore, the performance of the TEC module is based on several parameters that include: temperature of the hot and cold side of the TEC module; thermal and electric conductivity of thermoelement; electric contact resistance between the surface of the device and cold side of TEC; cooling capacity; the thermal efficiency which is termed as figure of merit (Z); the thermal resistance of the heat sinks on the hot side of TEC module; applied current at a couple of p-type and n-type thermoelement. The number of thermoelements in the TEC module depends upon the cooling efficiency requirement and the maximum current [6].

Over time researchers have focused on either developing new thermoelectric cooling techniques or improving existing TEC techniques for better performance. For example, Chein and Chen [7] performed a theoretical and experimental study of TEC performance for cooling a refrigerated object. Furthermore, Zhou [8] analyzed the theoretical model for optimizing the performance TEC system regarding COP and cooling capability of the TEC system. Moreover, an experimental investigation was carried out to examine the effect of COP and other cooling parameters by Yadollah et al. [9] and Yakut [10] for the general application. Huang et al. [6] performed a theoretical and experimental study to examine the performance of the TEC cooling system for electronics cooling applications. Also, Naphon and Wiriyasart [11] carried out experiments to examine the effect of the thermoelectric system on the CPU. They observed a significant improvement for CPU cooling with and without the TEC system. Additionally, Khonsue [12] carried out the same experimental study, and the results indicate that the heat transfer rate increased with increasing coolant flow rate and higher channel. Ling et al. [13] investigated the thermal performance of a thermoelectric water-cooling device for the electrical component to analyze the effect of heat load and the cooler's current on the cooling performance of the thermoelectric module.

An experimental and theoretical investigation was carried out by Kobus and Oshio [14] to examine the thermal performance of the pin-fin heat sink. Furthermore, Lie et al. [15] carried out an experimental study to examine heat transfer and connected bubble characteristics of FC-72 on a micro pin-finned silicon chip. The experimental data indicate that adding a micro-pin fin structure to the chip surface effectively improves convection and heat transfer. A theoretical study of a TEC designed for small space cooling applications for the buildings was carried out by GIllot et al. [16] to find the maximum operating conditions; also, Maneewan et al. [17] and Cherkez [18] evaluate the cooling performance and thermal comfort of TE air conditioner based upon the cooling thermoelements. An experimental analysis of a mini-channel water-cooled thermoelectric refrigerator was carried out by Gokeck and Sahin [1] at different voltage and different flow rates of the cooling water in the mini channel. Riffat et al. [19] carried out an experimental analysis to examine the application of heat pipes and a phase change material (PCM) in thermoelectric refrigeration. The results indicate that the use of an encapsulated PCM enhances the performance of the system. It also provides storage capacity, which helps handle peak loads. Chein and Huang [3] carried out an experimental study to check TEC applications in electric cooling. To increase the performance of thermoelectric coolers, Karwa et al. [20] tried a low thermal resistance heat sink design with water-cooling integrated on the hot side of a thermoelectric refrigerator.

In this study, the TEC is integrated with the heat exchanger differently from the traditionally used way to examine the effect of the different parameters on the system performance. Several research studies have been carried out to check the performance of TEC with different types of the heat sink. Moreover, there are many applications and types of thermoelectric cooling systems that have been using so far. However, the authors found limited research work supporting the TEC with the cold plate and heat sink used for the cooling application [21]. In this work, the heat sink was used to spread the cooling effect instead of heat spreading, which is generally used in TEC applications. Apart from that a cold plate heat exchanger was used for the heat removal from the hot side of the TEC module. Moreover, a copper tube heat was used to remove the heat from the hot liquid coming out of the cold plate heat exchanger and release it to a closed insulated room. Therefore, the copper tube heat exchanger was placed inside the closed room. Moreover, the liquid just released some heat to the closed room goes back to the chiller for further cool down. The present work investigates the system's cooling performance by using different parameters such as input current, liquid flow rate, inlet air fan speed, etc.

2. Working Principle of TEC System

The proposed thermoelectric cooling system is based upon the Peltier effect as described earlier in the Introduction. A thermoelectric unit is made up of p-type and n-type semiconductors connected by a good conductive material. Semiconductors are electrically connected in series and thermally in parallel, combined with two ceramic plates forming a single-stage cooler's hot and cold side. When it places across the finite temperature difference, a voltage difference is created, known as the Seebeck effect. When an electric current passing through one or more pairs of elements, a finite temperature difference is created between two junctions. Since one junction absorbs heat from the environment; therefore, the temperature at one junction is lower than ambient. Whereas the absorbed heat is carried along with the elements by electron transport as they move from low to high energy state, the temperature at that junction is higher than the ambient temperature. This combined effect is known as the Peltier effect. The mathematical representation of the Peltier effect can be written as $Q = \pi I$, whereas Q is defined as Peltier heat and as Peltier coefficient, and I as a thermal current. However, the cooling performance of the single module is minimal and cannot be used for practical application. Therefore, an array of such units is connected thermally in parallel and electrically in series to generate a thermoelectric effect [2].

3. Mathematical Modeling

A mathematical model is developed for the system that includes the heat removal rate of various components and interfaces. The proposed model is divided into three subdivisions such as: (i) a model for the thermoregulator part; (ii) a model for the closed room system; (iii) a model for the primary TEC cooling system. For the mathematical analysis, the cold plate heat exchanger inlet and outlet temperature are considered as $T_{CPI,1}$ and $T_{CPO,1}$, respectively. The heat removal rate of the cold plate heat exchanger is calculated using the given formula for both the top and bottom sides:

$$\dot{Q}_{H,TEC1} = \dot{Q}_{loss1} + \dot{m}_w C_{pw}(T_{CPI,1} - T_{CPO1}) \quad (1)$$

where $\dot{Q}_{H,TEC1}$, $\dot{Q}_{loss1}$, $\dot{m}_w$, C_{pw}, $T_{CPO,1}$, $T_{CPI,1}$ are heat removal rate from hot side of the TEC module, total heat loss from top side, mass flow rate of water (=density of water $\times$ volume flow rate of water) inside cold plate heat exchanger, specific heat of water, cold plate outlet temperature and cold plate inlet temperature for the top side of the TEC cooling system, respectively.

Figure 1 presents schematically the overall energy flow in the system.

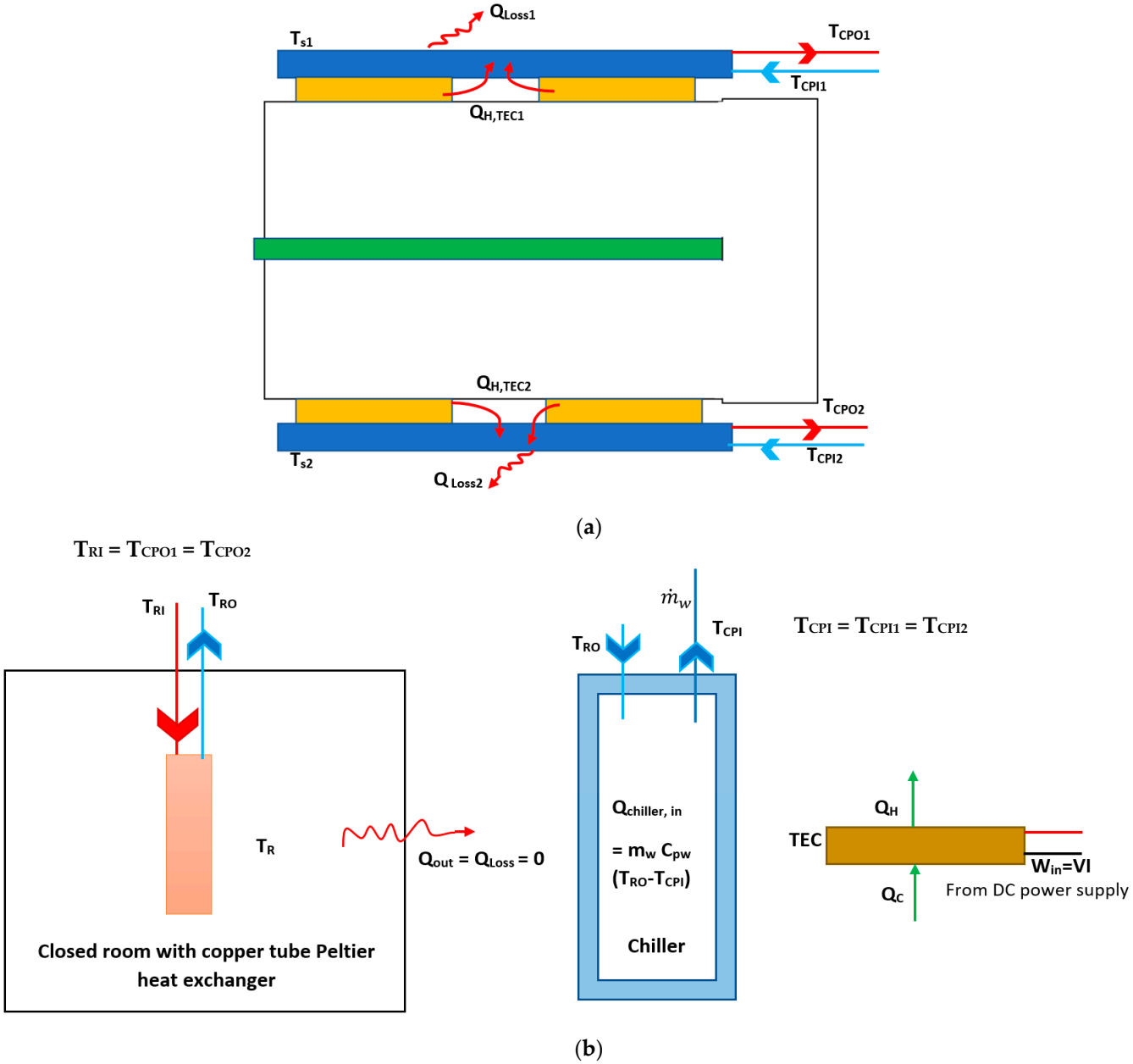


Figure 1. Schematic diagram of show the energy flow of the system (**a**) TEC with cold plate and air channel, (**b**) chiller and closed room with copper heat exchanger.

The heat loss from the top side of the clod plate is calculated using the following equation:

$$Ra_L = G_r P_r \tag{2}$$

where for natural convection Ra_L (product of Grashof and Prandtl number), G_r and P_r are Rayleigh number, Grashof number, and Prandtl number, respectively. The Nusselt number can be obtained from:

$$Nu = 0.13 {Ra_L}^{1/3} \tag{3}$$

where Nu is Nusselt number which is used to find the heat transfer coefficient.

$$Nu = \frac{hL}{\lambda} \tag{4}$$

where h, L, and λ are heat transfer coefficient, length of the cold plate heat exchanger, and thermal conductivity, respectively. The heat loss from the top side of the surface can be calculated as:

$$\dot{Q}_{loss1} = hA_s(T_s - T_\infty) \quad (5)$$

where $\dot{Q}_{loss}$, A_s, T_s and T_∞ are total heat loss from the top surface, surface area of the cold plate heat exchanger, surface temperature of the cold plate, and ambient temperature of the room. However, to find the total heat removal rate of the bottom surface, it can be written as:

$$\dot{Q}_{H,TEC2} = Q_{loss2} + \dot{m}_w C_{pw}(T_{CPO,2} - T_{CPI,2}) \quad (6)$$

where $\dot{Q}_{H,TEC2}$, $\dot{Q}_{loss2}$, $\dot{m}_w$, C_{pw}, $T_{CPO,2}$, $T_{CPI,2}$ are heat removal rate from hot side of the TEC module at the bottom, total heat loss from bottom side, mass flow rate of water (= density of water × volume flow rate of water) inside cold plate heat exchanger, specific heat of water, cold plate outlet temperature and cold plate inlet temperature for the bottom side of the TEC cooling system, respectively. Equation (6) is similar for the bottom surface; however, the Nusselt number for the bottom hot surface is:

$$Nu = 0.27{Ra_L}^{1/4} \quad (7)$$

Therefore, the heat loss for the bottom hot surface is calculated using the same equation as Equation (5). However, the total heat removal rate is equal to the summation of the heat removal rate from the top and bottom surface, which is equal to the sum of Equations (1) and (6):

$$\dot{Q}_{H,TEC} = \dot{Q}_{H,TEC1} + \dot{Q}_{H,TEC2} \quad (8)$$

where $\dot{Q}_{H,TEC}$ is total heat removal rate from the hot side of top and bottom surface of the cold plate heat exchanger. To find the heat removal rate from the cold side of the TEC module, the following equation is used:

$$\dot{Q}_C = \dot{Q}_{H,TEC} - W_{in} \quad (9)$$

where $\dot{Q}_C$ is heat removal rate from the cold side of the TEC. Here, Win is the energy required by the TEC modules to provide the Peltier effect. The energy required by fans and other item of the system are not included in Win, therefore the COP is not the coefficient of performance of the whole system, but only of the TEC modules. The performance of the TEC module can be calculated if the total supplied power in Equation (10) and heat removal rate of the cold plate is known; therefore, the equation is used:

$$\text{COP} = \frac{\dot{Q}_C}{W_{in}} \quad (10)$$

where COP is the coefficient of performance which mainly depends upon the input current to the system. From the above equation derivation, the heat removal rate and coefficient of performance largely depend upon the input current to the system as well as the TEC. The maximum performance can be achieved by optimizing the input current.

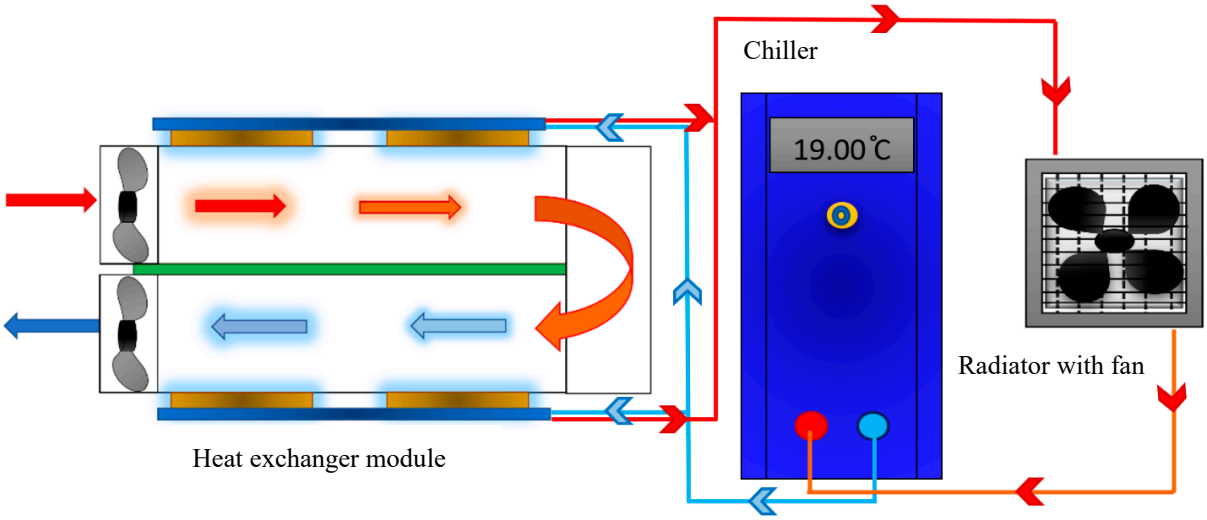
4. Experimental Components and Setup

A detailed experimental setup is presented in this section (as shown in Figure 2). The experimental setup consists of thermoelectric cooling (manufactured by Tellurex, Traverse, MI, USA) module to create a cooling effect, a cold plate (model: CP15G05, manufacturer: LYTRON, Woburn, MA, USA) to remove heat from the hot side of the TEC module, copper tube fin heat exchanger (model: LC200, manufacturer: TE Technology, Traverse; MI, USA) to remove heat from the liquid to deliver cool liquid to the chiller (manufacturer: Polystat, Montreal, QC, Canada) with precision temperature controlled to supply water to the cold plates, K-type thermocouple (manufacturer: Omega, St-Eustache, QC, Canada) and 16-

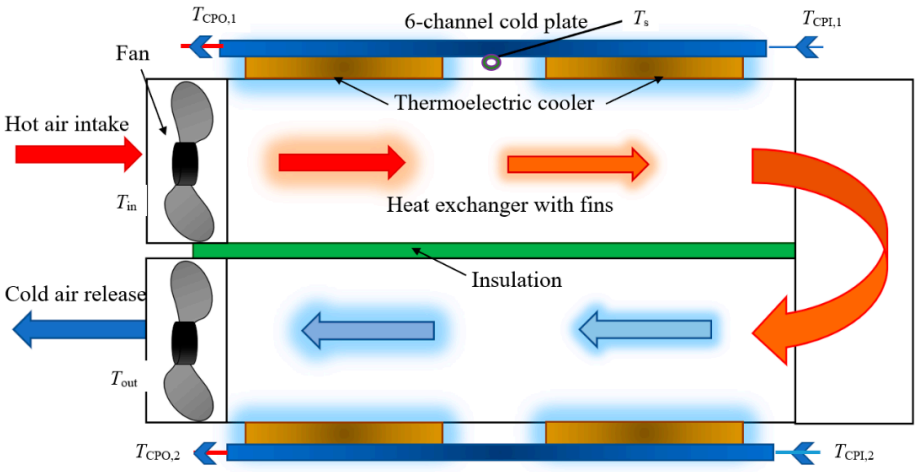
channel NI-DAQ system (manufacturer: National Instruments, Austin, TX, USA). The main aim of the proposed design is to supply the ambient air to the heat sink sandwiched by TEC module on both the side of the heat sink to generate cool air. Furthermore, the hot liquid from the cold plate is passed to the copper heat exchanger, which is inside in an insulated closed room made from styrofoam and supply cool liquid back to the chiller. Therefore, the temperature at various points is monitored during the operation of the system (see Figure 2). A detailed description of each component is given in the following sections.

4.1. Cold Plate Configuration

To remove the heat from the hot side of the TEC module during the system's operation and enhance the TEC module's performance, cold plates (manufacturer: LYTRON), made of aluminum, were used. The cold plate has eight through holes (diameter: 10 mm) that carry copper pipes (total length: 1940 mm) as shown in Figure 2c. Two cold plates were used, one on the top side and another one on the bottom side of the heat sink. The hot side of the thermoelectric modules is connected to the cold plate, which absorbs the heat released from the thermoelectric module. Table 1 lists the thermophysical properties of the used cold plate.



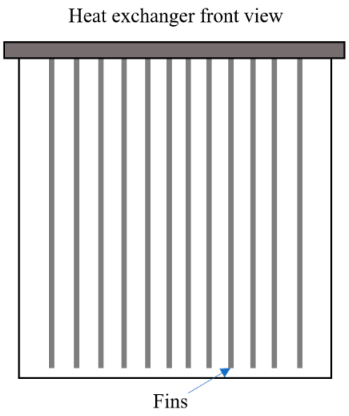
(**a**)



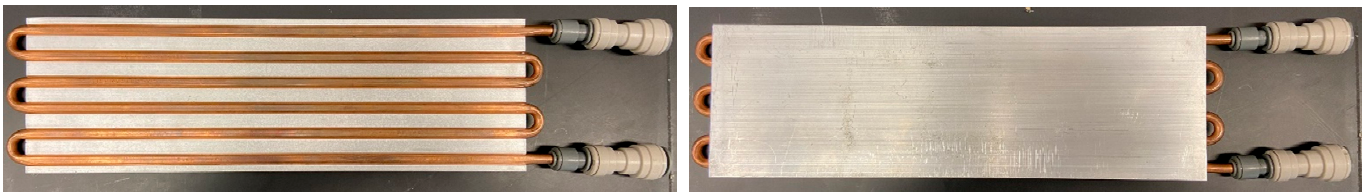
(**b**)

Figure 2. *Cont.*



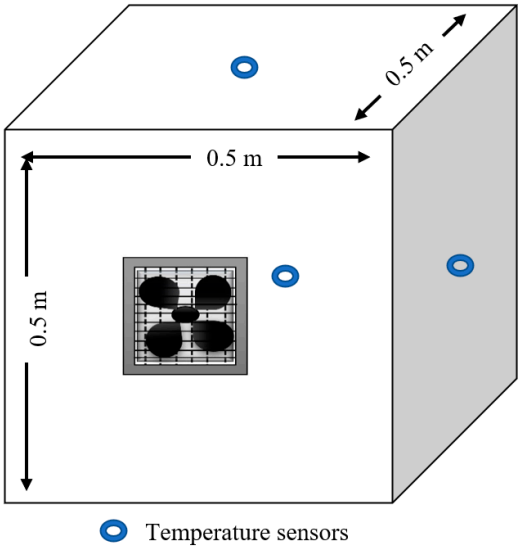


(**c**)



(**d**)





(**e**) (**f**)

Figure 2. *Cont*.



(**g**)

Figure 2. (**a**) Schematic presentation of the experimental setup, (**b**) details of heat exchanger module, (**c**) front view of heat exchanger with vertical fins, (**d**) cold plate, (**e**) copper tube Peltier heat exchanger, (**f**) insulated room with temperature sensors and heat exchanger, (**g**) Extended U-section enclosure.

Table 1. Thermophysical properties of the cold plate used in the experiment.

Specification	Values
Dimension	304.8 mm × 95.3 mm
Thickness	7.6 mm
Configuration	6-Pass
Max. Pressure	10 bar
Max. Flow Rate	4 lpm

Both cold plates are firmly attached to the TEC with the help of nuts and bolts for proper contact and heat dissipation. In addition, K-type thermocouples are attached to the surface of the cold plate, which is in contact with the TEC to investigate the heat removal rate from the cold plate. Moreover, thermal paste is applied between the TEC module and cold plate connection to decrease the thermal resistance.

4.2. TEC Module Configuration

A single-stage thermoelectric cooling module C2-55-2812 (company Traverse; MI, USA) was used to generate the cooling effect designed explicitly for high-volume cooling applications. Thermoelectric cooler works on the principle of the Peltier effect to generate a heat flux between the junction of two different materials. TEC module is made up of semiconductor material such as bismuth telluride, having a length of 55 mm, a width of 55 mm, and a height of 3.75 mm. The TEC module pressed between two heat spreading metal surfaces made up of aluminum- one on the hot side and another on the cold side. The cold side of the TEC module is attached with the plate type of heat sink to generate a cooling effect inside. The hot side is attached to the cold plate to remove generated heat. Table 2 gives a detailed description of the TEC characteristics.

Table 2. Performance specification of thermometric module.

Performance Specification	Values	
(Hot Side)	**T_{Hot} 27 °C**	**T_{Hot} 50 °C**
DT_{max} °C	68	76
V_{max} (V)	28.1	31.5
I_{max} (A)	12.0	12.0
$Q_{c\ max}$ (W)	224.0	245.6
AC Resistance (Ω)	2.10	2.35

4.3. Copper Tube Fin Heat Exchanger

A copper tube fin heat exchanger is used to provide cooling to the heat source (see Figure 2e). The basic working principle is simple: fluid flows through the inlet, gets cooled, and flows out from the outlet. Moreover, the fan attached to fin releases hot air to the environment. In this experiment, the copper tube fin heat exchanger aims to remove heat from the cold plate liquid and provide a cold liquid back to the thermo-regulator. Therefore, the outlet of both the cold plates are connected as an inlet to the heat exchanger, and an outlet of the heat exchanger is connected as an inlet to the thermo-regulator.

Since the heat exchanger provides hot air; therefore, this hot air can be used for heating purpose in any application where needed. Hence. the heat exchanger is attached in the closed room ($0.5 \times 0.5 \times 0.5\ m^3$) made up of styrofoam (1 inch thick). So, when the fan releases hot air, it creates a hot temperature inside the closed room. The heat exchanger has a length of 254 mm, width 161 mm, and height of 13.5 mm. The performance specification of the heat exchanger is given in Table 3.

Table 3. Performance specification of the Peltier thermoelectric cooler.

Performance Specifications	Values
TE max. power	24VDC at 17.3 A
External fan power	24VDC at 0.3 A
Liquid flow rate	1.6 L/min
Max. liquid pressure	205 kPa

4.4. Heat Sink

The heat sink is a passive heat exchanger to transfer the heat. Generally, the heat sink is attached to the component releasing heat to dissipate heat to the surroundings to prevent overheating. However, for this experiment, the heat sink is used to absorb the heat from the incoming air and as a result the air coming out from the channel becomes cold. In this experimental setup, two heat sinks are used; both are firmly attached back-to-back to pass the airflow from one of the sinks to the other via an extended U-section. The cold side of the TEC is attached to the heat sink in order to absorb the heat from the incoming air. A fan is attached at the opening of the top heat sink to provide airflow to the heat sink. In addition, another fan is attached to the bottom heat sink to suck the cold air from the channel and release it to the surrounding environment. Two K-type thermocouples are attached, one at the opening of the bottom heat sink, to measure the temperature of inlet airflow. Another one is attached to the top one to measure the temperature of air coming out from the heat sink. The heat sink has a length of 335 mm, a width of 128 mm, and a height of 135 mm each.

4.5. Extended U-Section Enclosure

The extended U-section comprises a transparent acrylic sheet having a length of 128.5 mm, a width of 16.5, and a height of 278 mm. To provide a curve shape inside the U-section, styrofoam was used, and after that reflective bubble, a sheet was used to provide a smooth path for the air. U-section provides a path for the air to flow from the top sink heat sink to the bottom. A photograph of an extended U-section is in Figure 2g.

4.6. Overall Experimental Setup

The experimental procedure was carried out at various stages. A prototype of a thermoelectric cooling system was designed to provide cool air at a certain temperature using a TEC technology that connected to the DC power source (as required see Table 3). As cold plates are used to remove the heat from the hot side of the TEC module, the cold plate outlet is connected to the liquid cooler to cool down the liquid again. The current experimental setup serves two purposes (i) To provide cool air (5 °C to 22 °C) at various parameters; (ii) To provide hot air (22 °C to 28 °C) to the insulated room as a byproduct. The TEC module's side extended U-section, inlet, and final temperature at the heat sink is measured using K-type of thermocouples to test the performance of the developed system. Three thermocouples are attached to the insulated room (size of the room is $0.5 \times 0.5 \times 0.5$ m^3) at different points to measure the temperature (see Figure 2e). First, the system's performance was examined at a different applied current of 2, 3, 4, 6 and 8 A to measure the effect on the cooling mechanism. In the next experiment series, the current will remain fixed at 4A, and the speed of the inlet air flow rate will change to 2.25, 2.55 and 3.55 m/s. Lastly, the inlet water flow rate will be changed while keeping the current at 4A and the inlet air flow rate at 2.25 m/s. The reason behind choosing input current and inlet air flow to be fixed was to investigate the effect of these parameters' on the system behavior. The water flow rate varies to 3.04, 2.16 and 1.80 L/min. Figure 1 shows the overall experimental setup with details of three major modules: heat exchanger module, chiller, and radiator with fan.

Two power supplies were used, and the supply current to the TEC was adjusted manually for supplying required power input to the system. After all the components were secured on the position, the NI DAQ data acquisition system was activated. K-type of thermocouples were used to record the temperature at the various point every 5 s. Finally, during the experiments mentioned above, the whole setup was thermally insulated to minimize losses due to conduction and convection to the surrounding. For the even comparison, the initial temperature of the thermoelectric cooling system was kept at room temperature (i.e., 20 °C–23 °C). After the equilibrium ambient conditions, power supplied to the TEC, inlet fan, and Peltier thermoelectric cooler was turned on.

5. Experimental Tests Results, and Discussion

In this section, the results were selected related to the effect of various parameters on the cooling effect, such as the effect of different input currents, the effect of various air inlet flow, and various water flow rates to the cold plate. Furthermore, the effect of the parameters as mentioned above on the Peltier thermoelectric liquid cooler inside the closed room is also measured.

5.1. Effect of Input Current to TEC

The cooling effect generated by the TEC module depends upon various parameters such as supply current, heat removed from the hot surface. However, the cooling effect is largely depending upon the applied current to the TEC module. Different current inputs of 2, 4, 6 and 8 A have been applied to the TEC to examine the performance of the TEC system. Figure 3 shows the temperature distribution of the system. As more current is applied to the TEC, a large amount of cooling effect is generated by TEC.

The cooling temperature varied from 16 °C to 9.2 °C when the input current to the system is varied from 2 A to 8 A. It is also observed that the cooling effect increased with increasing the supply current to the TEC. Table 4 gives cooling temperature values at various times.

As the TEC draws more current from the supply, it generates a more cooling effect on the cold side, leading to decreased temperature. As the current increased from 2 A to 8 A, a maximum 40% decrement in the temperature was observed. Furthermore, the bulk mean temperature of the water inside the cold plate is plotted to cool down the temperature at the different applied currents. The bulk mean temperature is used to calculate the heat

removal from the cold plate. In this case, to measure the bulk mean temperature, the inlet, and outlet of cold plate piping were recorded (as shown in Figure 2b). The average of the top and bottom cold plate inlet and outlet gives bulk mean temperature. Figure 4 gives bulk mean temperature distribution against time for various applied currents.

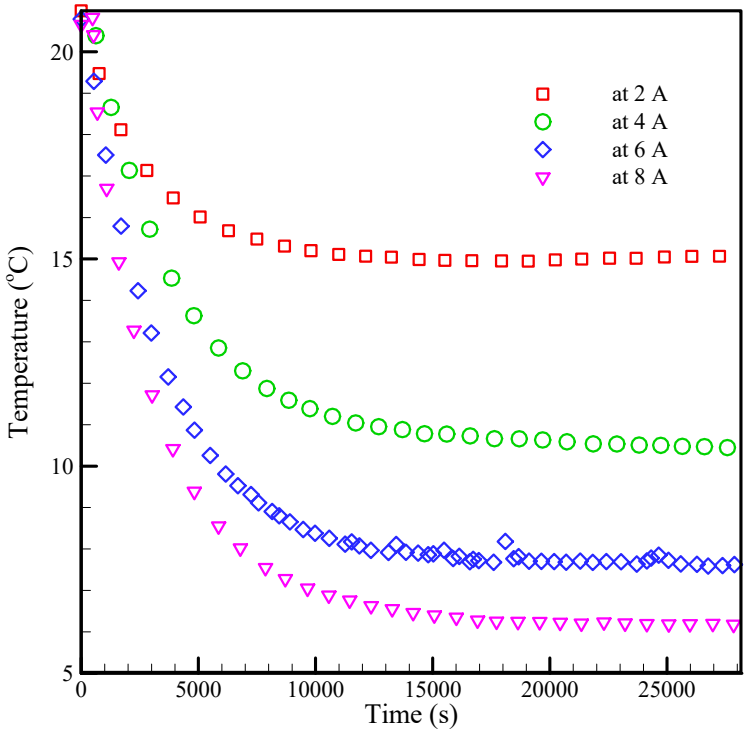


Figure 3. Final cooling temperature at various inlet currents of 2A, 4A, 6A, and 8A.

Table 4. Temperature values at various applied currents to thermoelectric.

Time (s)	2 A	4 A	6 A	8 A
5000	16 °C	13.4 °C	10.6 °C	9.2 °C
10,000	15.2 °C	11.3 °C	8.4 °C	6.8 °C
15,000	14.9 °C	10.7 °C	7.9 °C	6.4 °C

The total heat removal rate combined from the top and bottom surface of the cold plate is plotted as a function of time in Figure 5.

The heat removal rate is calculated using Equation (8) in the mathematical model. It is observed from the graphs that the heat removal rate increases with the increasing applied current to the TEC module from 2A to 8A. As the TEC module draws more current from the supply, the temperature on the hot side of the plate also increases with the increment to the current. That leads to more amount of heat carried out by the fluid inside the cold plate. However, it is observed from Figure 5 that the heat removal rate remains constant for the specifically applied current during the whole experiment.

The amount of heat removal rate from the cold side of the cold plate heat exchanger is plotted against time in Figure 6. The calculation for the heat removal rate from the cold side of the plate is mentioned in the mathematical model. Figure 6 indicates that the heat removal rate at first increases with time, and after that, it remains constant during the whole experiment. It can be observed that the heat removal rate from the cold side is less compared to Figure 5, which is the heat removal rate from the hot side of the cold plate. Since the cold side of the cold plate is in contact with the TEC module's cold side, there is a negligible amount of heat generated during the experiment. Still, the heat removal rate increased from 10 to 400 W as the applied current increased from 2 to 8 A.

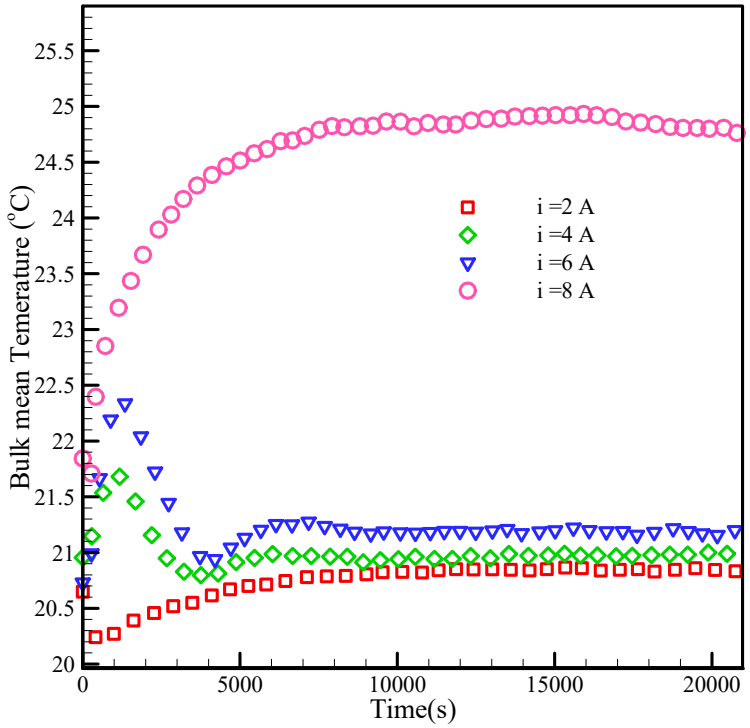


Figure 4. Bulk mean temperature for various input currents for the cold plate exchanger.

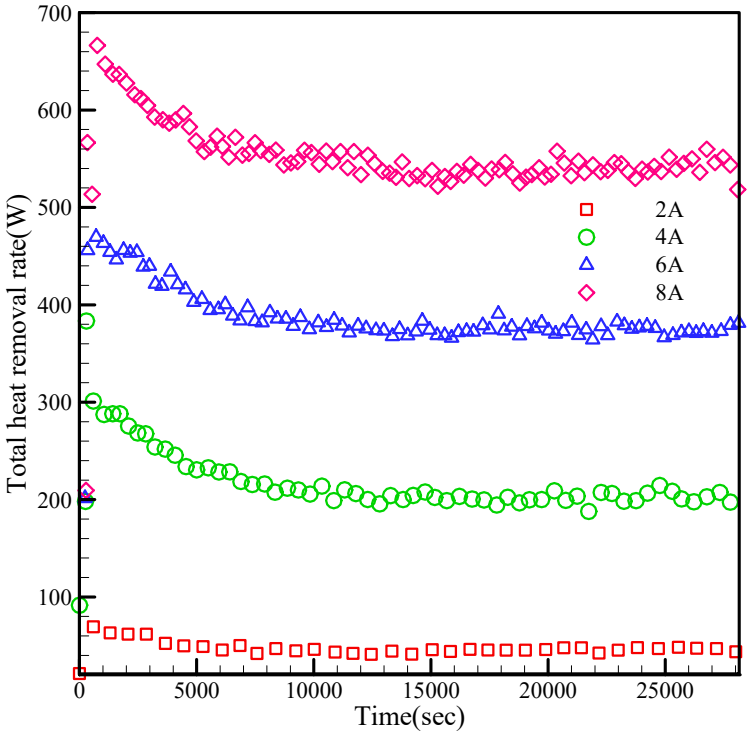


Figure 5. Total heat removal rate at various input currents from the hot side of the TEC module.

The coefficient of performance (COP) is plotted in Figure 7 using Equation (10) to examine the system's performance. It is observed that the COP of the system increases with increasing the applied current to the TEC modules. The current was varied from 2 A to 8 A, and as a result, the COP increased from 0.35 to 2 with different current inputs. The best result was recorded at an input current of 4 A where a COP of nearly 2 was calculated.

The COP of the system largely depends upon the heat removal rate and cooling effect generated by TEC modules.

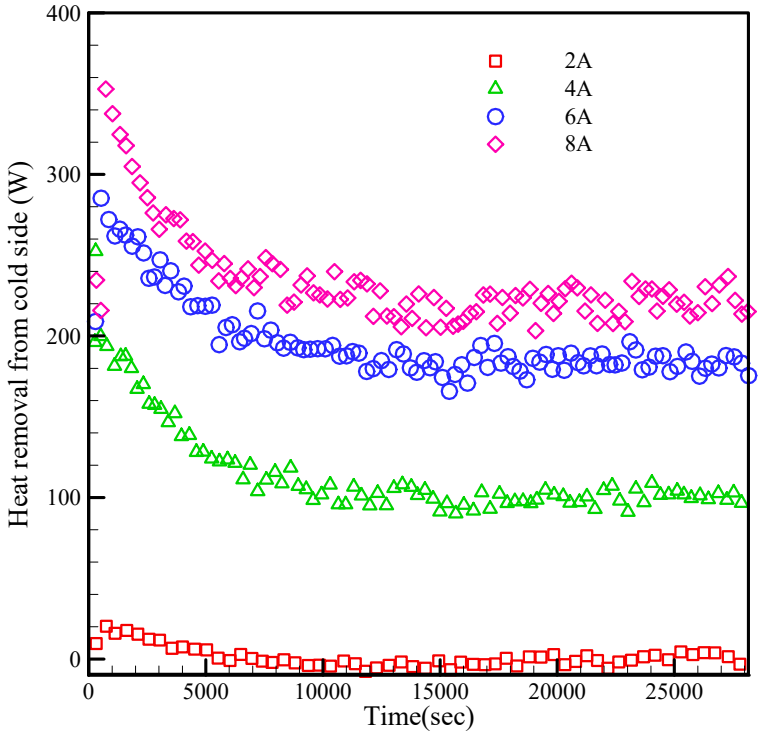


Figure 6. Total heat removal rate at various input currents from the cold side of the TEC module.

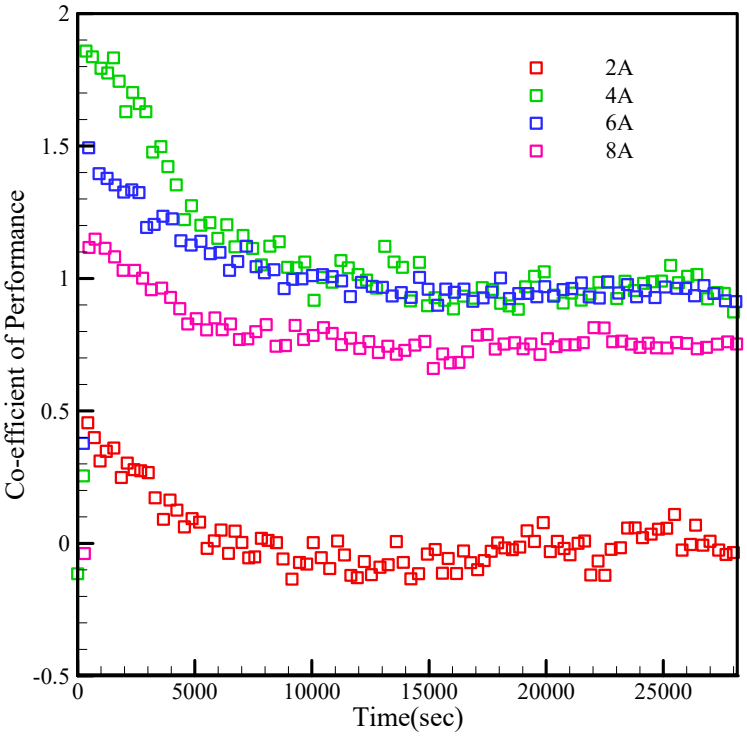


Figure 7. COP of the system at various input currents to the TEC module.

Additionally, Figure 8 presents the temperature distribution inside the closed room when the current varies.

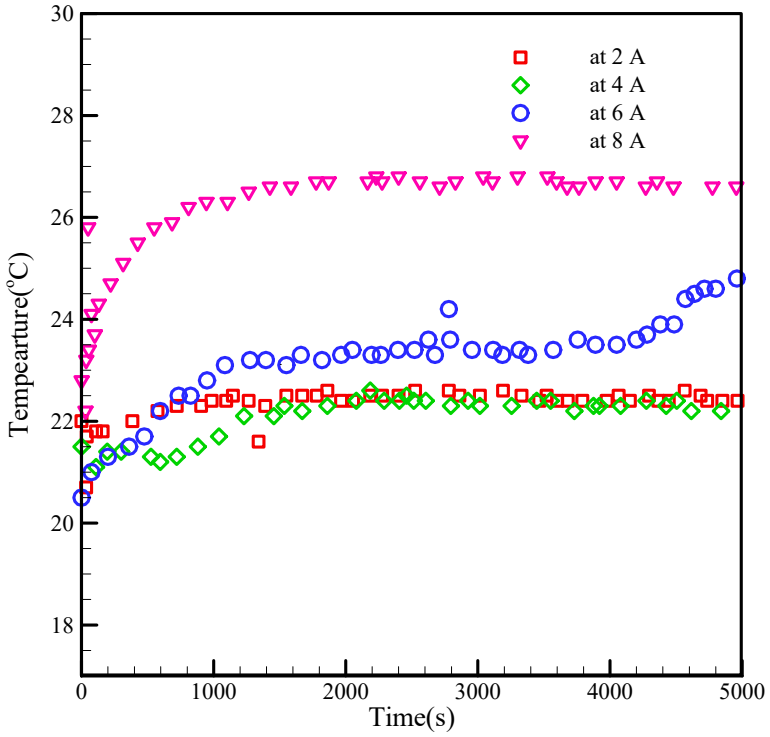


Figure 8. Temperature distribution by copper tube fin heat exchanger inside the closed room at various input current to the TEC module.

The TEC generates more cooling effect on the cold side as applied current increases, and the temperature on the hot side is also increased to maintain the temperature difference constant. Hence, this leads to generate a higher temperature on liquid inside the cold plate that removes heat from the hot side of TEC. Therefore, the thermoelectric liquid cooler releases more heat to the flowing liquid which ultimately increases the temperature inside the closed room.

5.2. Effect of Fan Speed

The inlet air flow rate of the fans, attached to the top and bottom channel (see Figure 3), is also one of the important parameters which affect the cooling effect. For the beginning, the applied current is kept constant at 4 A, and fan speed varies at different values. The graph of various fan speeds is plotted in Figure 9.

It can be observed from Table 5 that the cooling effect is not significant as the fan speed increases. The temperature is almost constant at the maximum fan speed. Furthermore, the temperature distribution inside the closed room did not show any significant change in the temperature. The reason behind high temperature is that as the airflow rate increases, it is not getting enough time to contact the cold surface, so to improve the cooling effect of the system, an appropriate inlet airflow is required, which can be measured by the trial-and-error method. It was observed that 58% temperature rose when the airflow rate increased from 2.35 m/s to 3.55 m/s.

However, for the bulk mean temperature, it can be observed from the graph that there is no significant effect at different inlet airspeeds. It is clear from Figure 10 that the bulk mean temperature is almost similar at the different fan speeds. Initially, the temperature rises, and after that, it falls and remains constant for the rest of the time.

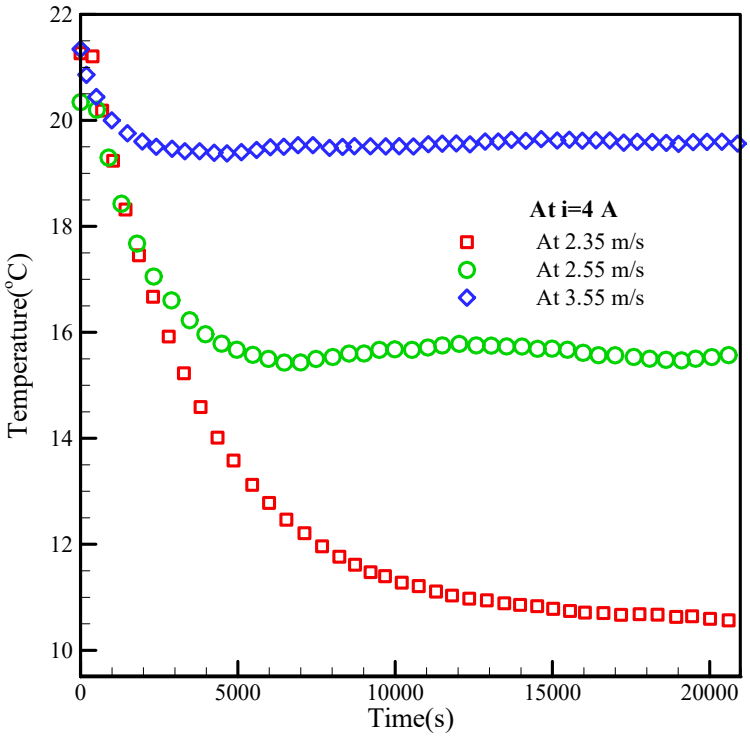


Figure 9. Effect of various inlet air flow rate on the final cooling temperature.

Table 5. Temperature values at various inlet air flow rate.

Time (s)	2.35 m/s	2.55 m/s	3.55 m/s
5000	13.4 °C	15.6 °C	19.3 °C
10,000	11.3 °C	15.4 °C	19.5 °C
15,000	10.7 °C	14.9 °C	19.6 °C

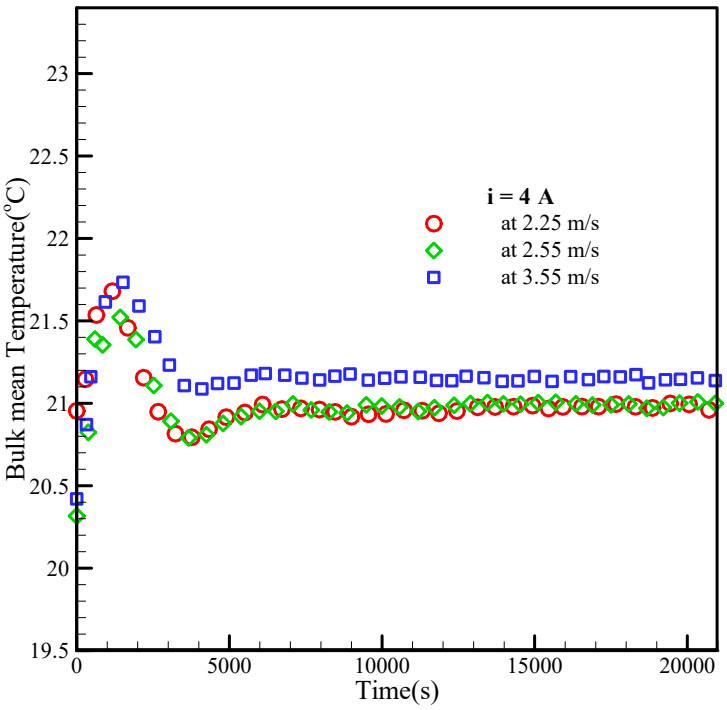


Figure 10. Bulk mean temperature at various inlet air flow rate.

The overall heat removal rate from the hot side of the cold plate is plotted in Figure 11.

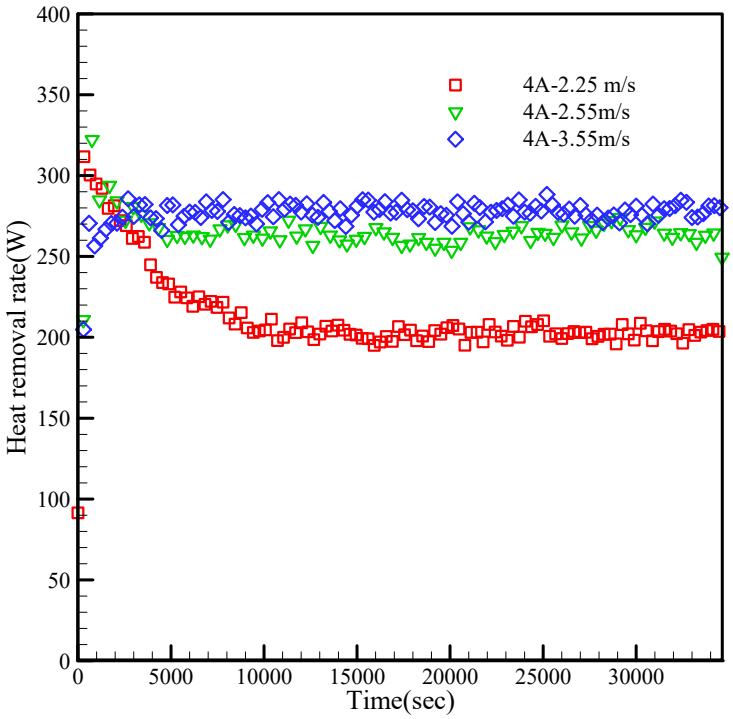


Figure 11. Total heat removal rate from the hot side of the TEC module at various inlet air flow rates.

It can be observed from the graph that the heat removal rate increases with increases in the fan speed. Furthermore, as the fan speed increase from 2.25 to 3.55 m/s the heat removal rate from the hot side of the cold plate is increases from 230 to 283 W at 5000 s, which shows 20% increment in the heat removal rate with an increase in the fan speed.

Figure 12 shows the heat removal rate from the cold side of the cold plate as a function of the time. It also follows the same pattern from the hot side of the cold plate. The heat removal rate increases with an increase in the fan speed. The heat generated by the cold plate is removed rapidly as the fan speed increase. At the beginning of the experiment, the heat removal rate increases as time goes; however, after a certain time, it will remain constant. Moreover, the heat removal rate increases from 127 to 179 W as the fan speed increases at 5000 s, indicating an increment of 33% on the heat removal rate from the cold side. Furthermore, to investigate the system's performance, the COP graph is plotted, and from the graph, it can be observed that the graph follows the same pattern as shown in the above graphs for the heat removal rate.

The COP of the system is plotted as a function of time in Figure 13. The COP is calculated using Equation (10) mentioned in the mathematical model section. It is observed that the COP of the system increases from 1.23 to 1.74 as the fan speed is increased from 2.25 to 3.55 m/s. The COP of the system largely depends upon the heat removal rate and cooling effect generated by TEC modules, so as the heat removal rate increases, the cooling effect generated by the TEC module also increases, improving the performance of the system. As the fan speed increases from 2.25 to 3.55 m/s, the COP shows an approximately 34% increase in the system performance.

As for the closed room temperature, there is no significant change in the temperature at various fan speeds, as shown in Figure 14. The temperature inside the closed room is between 21 °C–23 °C for different speeds. Therefore, it can be concluded that there is no significant cooling effect when the applied current is constant, and the fan speed varies. After a certain point, the temperature remains constant for the remaining experimental cycle.

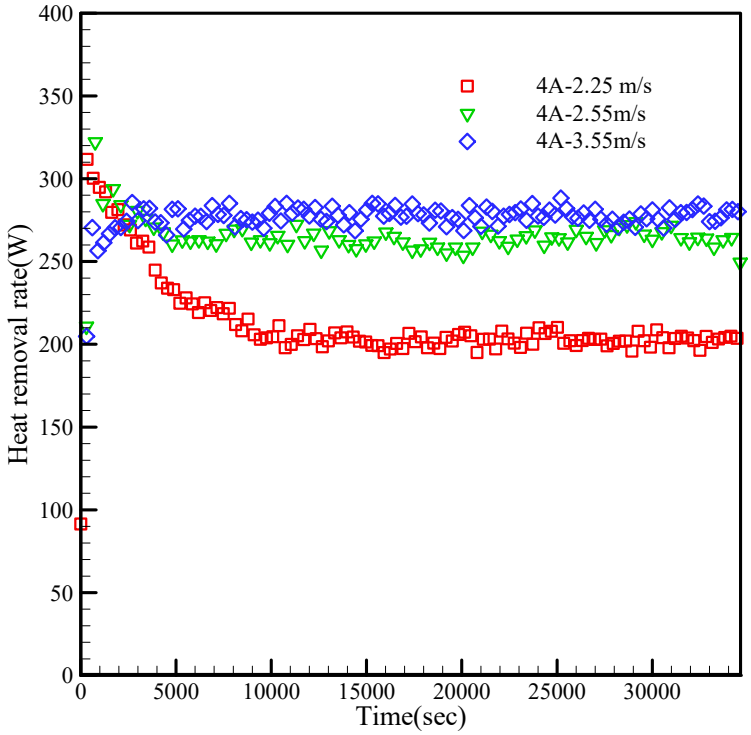


Figure 12. Total heat removal rate from the cold side of the TEC module at various inlet air flow rates.

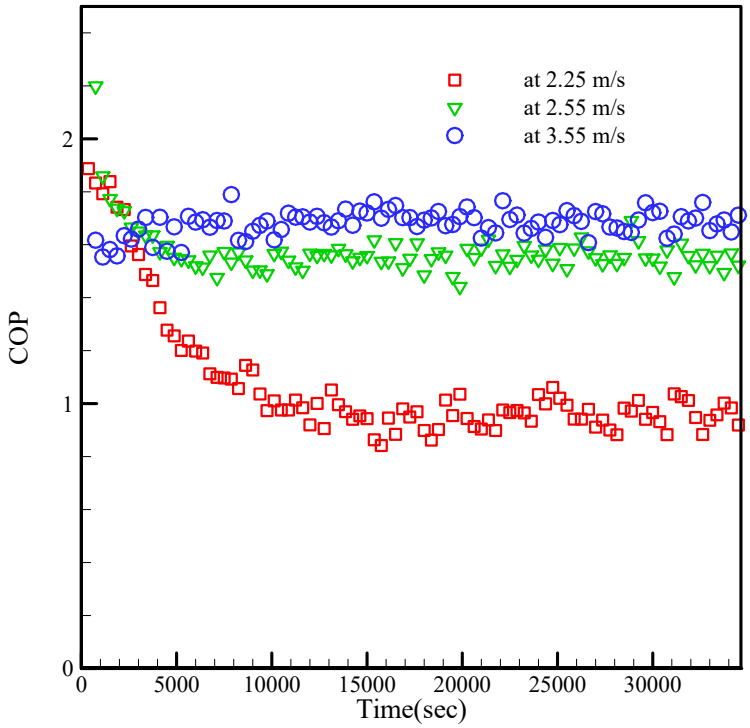


Figure 13. COP of the system at various inlet air flow rate.

5.3. Effect of Water Flow Rate on the Cold Plate

The water flow rate inside the cold plate and its effect on the final temperature is plotted as a function of time in Figure 15. The water flow rate was varied to 3.04, 2.16 and 1.80 L/min at a constant current supply of 4 A. It can be observed from Figure 14 that the temperature drops as the flow rate is decreased. Furthermore, the temperature at a different time is for the various water flow rate is presented in Table 6.

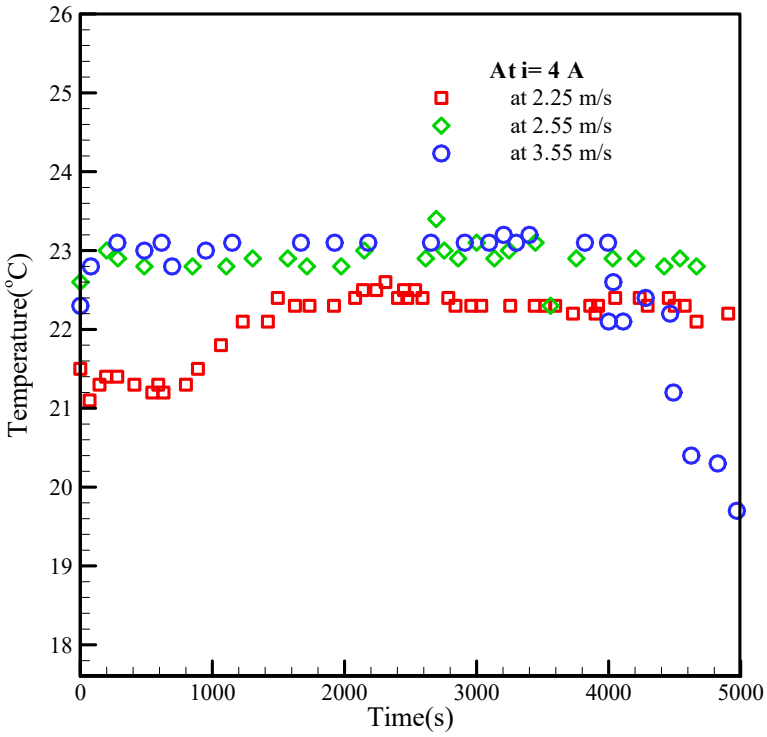


Figure 14. Temperature distribution inside the closed room at various inlet air flow rates.

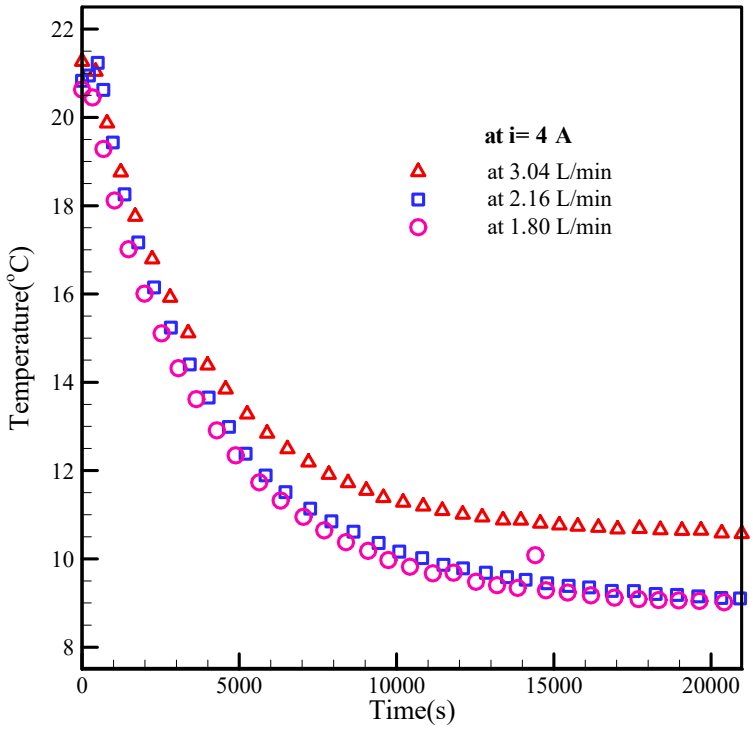


Figure 15. Temperature distribution at various water flow rates inside cold plate.

Table 6. Temperature distribution for various water flow rates inside the cold plate.

Time (s)	3.04 L/min	2.16 L/min	1.80 L/min
5000	13.4 °C	12.5 °C	12.2 °C
10,000	11.3 °C	10.1 °C	9.9 °C
15,000	10.7 °C	9.4 °C	9.2 °C

It can be observed from the table that the temperature decreased with a decrease in the water flow rate. One of the reasons for this can be that once the flow rate drops, it has more time to interact with hot surface and the heat removal rate increases as the amount of heat carried by the water increases based on the heat capacity of the liquid. Overall, there is a 15% decrease in the temperature noticed when the flow rate decreased from 3.04 to 1.80 L/min. Furthermore, there is no significant change for the bulk mean temperature when the flow rate varies (see Figure 16). Moreover, it maintained to lower temperature in the range of 20 °C–22 °C which also implies a good heat removal rate. Additionally, the graph follows the same pattern as variable fan speed; first, the temperature rises, then it drops to its minimum value, and finally, it remains constant.

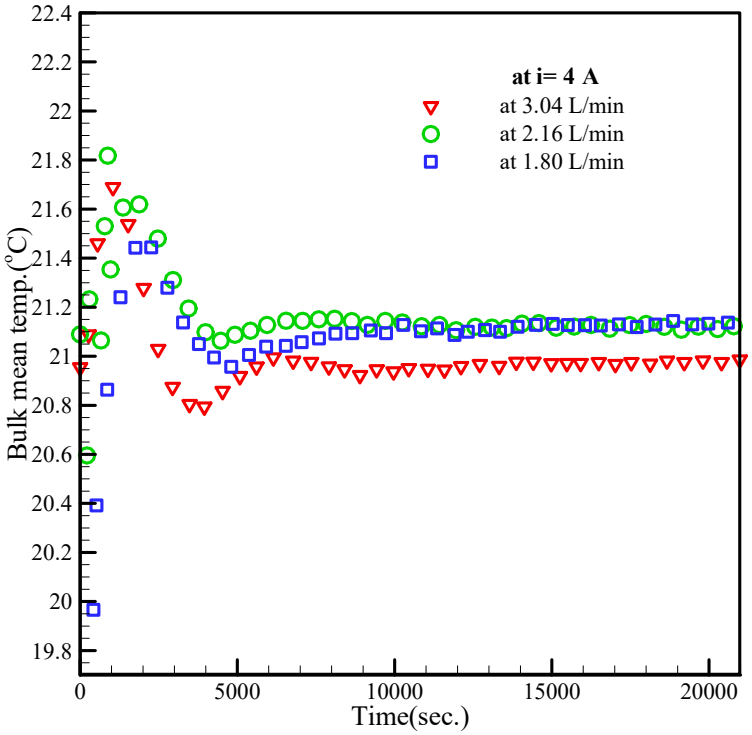


Figure 16. Bulk mean temperature at various water flow rates inside the cold plate.

There is no significant effect on the heat removal rate by changing the water flow rate inside the cold plate. The graph is plotted as a function of time for the closed room temperature in Figure 17. It can be observed that there is no significant change inside the temperature. The temperature is almost similar for the 2.16 and 1.80 L/min flow rates. However, the temperature varies between 21 °C–23 °C at variable water flow rate inside the cold plate changes from 3.04 to 1.80 L/min.

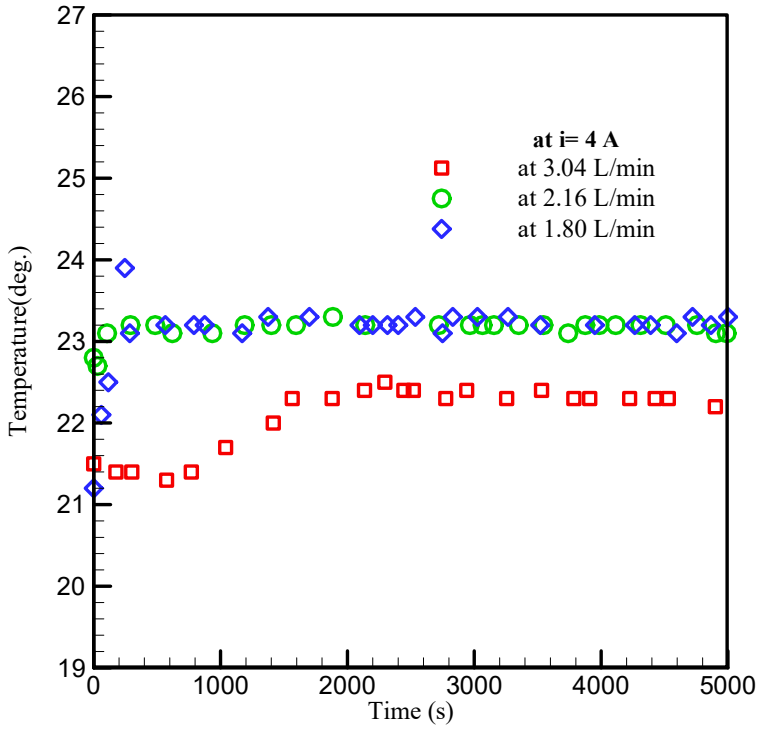


Figure 17. Temperature distribution inside the closed room during various water flow rates inside the cold plate.

6. Uncertainty Analysis

Data measuring is associated with uncertainty and depends on the accuracy of the devices used in the experiments. The following equation can calculate the uncertainty values based on the root mean square error (RMSE) method:

$$U = \sqrt{\sum_{0}^{i}\left(\frac{a_i}{x_i}\right)^2}$$

where U is the uncertainty of the experiment, a is the accuracy of the devices provided by the manufacturers, and x_i represents the measured values. The accuracy of the measurement devices is shown in Table 7.

Table 7. Accuracy of the measurement devices and the measure values.

Equipment	Accuracy (a_i)	Measured Values (x_i)	Relative Uncertainty ($\pm a_i/x_i$)
K-type thermocouples	±1 [°C]	Min: 0 °C Max: 105 °C	0.04 0.014
DAQ system	±0.02 [°C]	Min: 23 °C Max: 70 °C	0.0008 0.0002

Hence, the maximum uncertainty associated with the temperature measurements can be obtained as ±2%.

7. Cost Estimation

Table 8 presents a cost analysis of the proposed TEC-based cooling system and commercially available system. The table shows that the proposed prototype is cheaper (by approximately CAD300) than the commercial system available in the market.

Table 8. Cost analysis of the proposed TEC-based cooling system.

Component	Cost (CAD)
TEC module (4 Pcs)	15
Aluminum plate type heat sink (2 Pcs)	36
Inlet air flow pump	14
Cold plate heat exchanger (2 Pcs)	130
Copper tube heat exchanger	50
Water circulating pump	85
Additional cost	20
Total cost of the system	350
Available system in the market	600–700

8. Conclusions

The present work presents a new cooling design concept using TEC technology. This experimental investigation had two main objectives: (i) to cool down the air in an air duct channel for cooling purposes and (ii) then use the heat from the liquid coming out from the cold plate for heating purposes. Therefore, various parameters such as input current and water flow rates were varied to examine the effect on system behavior. Moreover, the aim was to cool down the air in the duck channel as low as possible and heating the insulated room as high as possible. Therefore, the cooling temperature was measured at various input currents 2, 4, 6 and 8 A at different inlet air temperatures and water flow rates inside the cold plate.

In the first set of experiments, it is observed that the cooling effect is increased upon increasing the current supplied to the TEC module. An approximately 40% cooling effect increase was seen while the applied current increased. Moreover, the temperature inside the closed room also shows a significant increment in its temperature. In the second set of experiments, the cooling effect decreases as the air inlet speed increases at various air inlet speeds. As the inlet airspeed was increased from 2.35 to 3.55 m/s, there was a rise in temperature of 58%.

Furthermore, there is no significant effect of inlet airflow rate for the bulk mean temperature. It is in the range of 21–22 for all different fan speeds. Besides, the cooling effect increases with a decrease in the water flow rate. It is noticed that the 15% cooling effect increased with a decrement of water flow rate from 3.04 to 1.80 L/min. Future work could be focused on using different liquids which have faster heat releasing and absorbing capacity than water

Author Contributions: Conceptualization, Y.P. and S.M.; methodology, Y.P. and A.R.M.S.; software, Y.P., A.R.M.S. and M.R.M.; validation, Y.P., A.R.M.S. and M.R.M.; formal analysis, S.M. and S.H.T.; investigation, Y.P.; resources, Y.P. and S.M.; data curation, Y.P., A.R.M.S. and M.R.M.; writing—original draft preparation, Y.P.; writing—review and editing, A.R.M.S. and M.R.M.; visualization, Y.P. and A.R.M.S.; supervision, S.M.; and S.H.T.; project administration, S.M.; funding acquisition, S.M. All authors have read and agreed to the published version of the manuscript.

Funding: This research received no external funding.

Conflicts of Interest: The authors declare no conflict of interest.

Nomenclature

A_s	Surface area of the cold plate heat exchanger (m^2)
C_{pw}	Specific heat of the water (kJ kg^{-1} K^{-1})
COP	Coefficient of performance
h	Convection heat transfer coefficient (W m^{-2} K^{-1})
$\dot{m}_w$	Mass flow rate of the water inside the cold plate heat exchanger (kJ s^{-1})
$\dot{Q}_{H,TEC}$	Heat removal rate at the hot side of the TEC (W)
$\dot{Q}_{loss}$	Rate of heat loss (W)
$\dot{Q}_C$	Heat removal rate at the cold side of the TEC (W)
T_{CPI}	Cold plate inlet temperature (°C)
T_{CPO}	Cold plate outlet temperature (°C)
T_S	Surface temperature of the cold plate at TEC hot side (°C)
$T\infty$	Ambient temperature (°C)
TEC	Thermoelectric cooling module
W_{in}	Total power supply to the system (W)
W_{TEC}	Power supply to the TEC modules (W)
W_{fan}	Power supply to the inlet air fan (W)
W_{HE}	Power supply to the copper tube fin heat exchanger (W)

References

1. Gokcek, M.; Şahin, F. Experimental performance investigation of minichannel water cooled-thermoelectric refrigerator. *Case Stud. Therm. Eng.* **2017**, *10*, 54–62. [CrossRef]
2. Alomair, Y.; Alomair, M.; Mahmud, S.; Abdullah, H.A. Theoretical and experimental analyses of solar-thermoelectric liquid-chiller system. *Int. J. Refrig.* **2015**, *56*, 126–139. [CrossRef]
3. Shourideh, A.H.; Ajram, W.B.; Al Lami, J.; Haggag, S.; Mansouri, A. A comprehensive study of an atmospheric water generator using Peltier effect. *Therm. Sci. Eng. Prog.* **2018**, *6*, 14–26. [CrossRef]
4. Eslami, M.; Tajeddini, F.; Etaati, N. Thermal analysis and optimization of a system for water harvesting from humid air using thermoelectric coolers. *Energy Convers. Manag.* **2018**, *174*, 417–429. [CrossRef]
5. Chein, R.; Huang, G. Thermoelectric cooler application in electronic cooling. *Appl. Therm. Eng.* **2004**, *24*, 2207–2217. [CrossRef]
6. Huang, H.-S.; Weng, Y.-C.; Chang, Y.-W.; Chen, S.-L.; Ke, M.-T. Thermoelectric water-cooling device applied to electronic equipment. *Int. Commun. Heat Mass Transf.* **2010**, *37*, 140–146. [CrossRef]
7. Chein, R.; Chen, Y. Performances of thermoelectric cooler integrated with microchannel heat sinks. *Int. J. Refrig.* **2005**, *28*, 828–839. [CrossRef]
8. Zhou, Y.; Yu, J. Design optimization of thermoelectric cooling systems for applications in electronic devices. *Int. J. Refrig.* **2011**, *35*, 1139–1144. [CrossRef]
9. Faraji, A.Y.; Goldsmid, H.; Akbarzadeh, A. Experimental study of a thermoelectrically-driven liquid chiller in terms of COP and cooling down period. *Energy Convers. Manag.* **2014**, *77*, 340–348. [CrossRef]
10. Yakut, K.; Alemdaroglu, N.; Kotcioglu, I.; Celil, C. Experimental investigation of thermal resistance of a heat sink with hexagonal fins. *Appl. Therm. Eng.* **2006**, *26*, 2264–2271. [CrossRef]
11. Naphon, P.; Wiriyasart, S. Liquid cooling in the mini-rectangular fin heat sink with and without thermoelectric for CPU. *Int. Commun. Heat Mass Transf.* **2008**, *36*, 166–171. [CrossRef]
12. Khonsue, O. Experimental on the liquid cooling system with thermoelectric for personal computer. *Heat Mass Transf.* **2012**, *48*, 1767–1771. [CrossRef]
13. Ling, Z.; Chen, J.; Fang, X.; Zhang, Z.; Xu, T.; Gao, X.; Wang, S. Experimental and numerical investigation of the application of phase change materials in a simulative power batteries thermal management system. *Appl. Energy* **2014**, *121*, 104–113. [CrossRef]
14. Kobus, C.; Oshio, T. Development of a theoretical model for predicting the thermal performance characteristics of a vertical pin-fin array heat sink under combined forced and natural convection with impinging flow. *Int. J. Heat Mass Transf.* **2005**, *48*, 1053–1063. [CrossRef]
15. Lie, Y.; Ke, J.; Chang, W.; Cheng, T.; Lin, T. Saturated flow boiling heat transfer and associated bubble characteristics of FC-72 on a heated micro-pin-finned silicon chip. *Int. J. Heat Mass Transf.* **2007**, *50*, 3862–3876. [CrossRef]
16. Gillott, M.; Jiang, L.; Riffat, S. An investigation of thermoelectric cooling devices for small-scale space conditioning applications in building. *Int. J. Energy Res.* **2009**, *34*, 776–786. [CrossRef]
17. Maneewan, S.; Tipsaenprom, W.; Lertsatitthanakorn, C. Thermal Comfort Study of a Compact Thermoelectric Air Conditioner. *J. Electron. Mater.* **2010**, *39*, 1659–1664. [CrossRef]
18. Cherkez, R. Theoretical studies on the efficiency of air conditioner based on permeable thermoelectric converter. *Appl. Therm. Eng.* **2012**, *38*, 7–13. [CrossRef]
19. Riffat, S.; Omer, S.; Ma, X. A novel thermoelectric refrigeration system employing heat pipes and a phase change material: An experimental investigation. *Renew. Energy* **2001**, *23*, 313–323. [CrossRef]

20. Karwa, N.; Stanley, C.; Intwala, H.; Rosengarten, G. Development of a low thermal resistance water jet cooled heat sink for thermoelectric refrigerators. *Appl. Therm. Eng.* **2017**, *111*, 1596–1602. [CrossRef]
21. He, W.; Yu, P.; Hu, Z.; Lv, S.; Qin, M.; Yu, C. Experimental Study and Performance Analysis of a Portable Atmospheric Water Generator. *Energies* **2019**, *13*, 73. [CrossRef]